

## Exclusive production at HERA

O. Lukina

M.V. Lomonosov Moscow State University, Skobeltsyn Institute of Nuclear Physics, Moscow, Russia

### Abstract

Recent studies of exclusive processes in  $ep$  scattering at HERA are presented. These include the results on exclusive dijets production and the measurement of the production ratio  $\psi(2S)/\psi(1S)$  in diffractive deep inelastic scattering, the first HERA measurement of  $\rho^0$  meson photoproduction with a leading neutron.

### Keywords

HERA; exclusive processes; photon; diffraction.

## 1 Introduction

The world only  $ep$  collider HERA operated at DESY, Hamburg, with electrons or positrons at 27.5 GeV and protons at 820 or 920 GeV during the years 1992 to 2007. Two collider experiments, H1 and ZEUS, collected data corresponding to an integrated luminosity of  $0.5 \text{ fb}^{-1}$  each. The high resolution multi-purpose detectors H1 and ZEUS equipped with additional forward sub-detectors allow for detailed analyses of exclusive processes, reviewed in this talk. These processes are clean experimentally, kinematic variables are fully reconstructed by measuring scattered electron and vector meson decay products or jets. Forward baryons ( protons and neutrons), which carry a large fraction of momentum of the incoming proton are detected with low acceptance by forward detectors.

The HERA facility can be viewed as a  $\gamma^*p$  collider, which allows measurements within a single experiment to be made over a wide range of the  $\gamma p$  centre-of-mass energy,  $W$ , up to its maximum value, set by the centre-of-mass energy of the electron-proton system  $\sqrt{s} = 310 \text{ GeV}$ . The photon virtuality,  $Q^2$ , ranged up to several thousand  $\text{GeV}^2$ . The reaction phase space can be divided into photoproduction ( $\gamma p$ ),  $Q^2 \approx 0 \text{ GeV}^2$ , and deep inelastic scattering ( DIS), where  $Q^2 > 1 \text{ GeV}^2$ . To describe the processes are used four momentum transfer squared at the proton vertex,  $t$ , Bjorken scaling variable,  $x_{Bj}$ , which is a fraction of proton’s momentum carried by struck quark, and also the fractional loss of proton longitudinal momentum,  $x_{IP}$ , and a fraction of Pomeron momentum ‘seen’ by photon,  $\beta = x/x_{IP}$ . At high energies as at the HERA collider the  $ep$  interaction is in fact an interaction of a virtual photon, emitted from the electron with the incident proton. Such processes is usually thought to proceed in two steps: interaction of the virtual photon with partons in the proton and the fragmentation of the intermediate partonic state into final hadrons. When the special configuration of the intermediate partonic state is small the former interaction is *hard* which implies possibility of the interaction within the perturbative quantum chromodynamics (pQCD), whereas the latter one is typical *soft* hadronic process, usually described by the phenomenological models. The precision of HERA data allows studies of exclusive processes in their transition from *soft* to *hard* interactions as well as in the pQCD domain.

## 2 Production of exclusive dijets in diffractive deep inelastic scattering

ZEUS Collaboration has reported on the first measurement of exclusive dijet production in high energy electron-proton scattering  $e + p \rightarrow e' + p' + jet1 + jet2$  with only dijet, electron and proton in the final state Ref. [1]. The process can be viewed as an interaction between the virtual photon,  $\gamma^*$ , and the proton, which is mediated by the exchange of a colourless object, Pomeron,  $IP$ , as it shown in Fig. 1. The production of exclusive dijets in DIS is sensitive to the nature of the object exchanged, therefore this measurement allows of different assumptions about the nature of diffractive exchange to be tested. The measurement is based on data collected with the ZEUS detector in 2003-2007 data-taking period

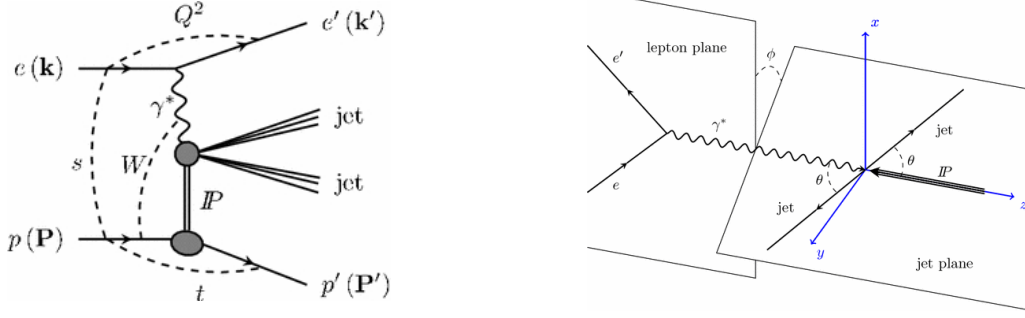


**Fig. 1:** (left) Schematic view of the diffractive production of exclusive dijets; (right) Definition of planes and angles in  $\gamma^* - IP$  centre-of-mass frame. The angle  $\phi$  is an angle between these two planes.

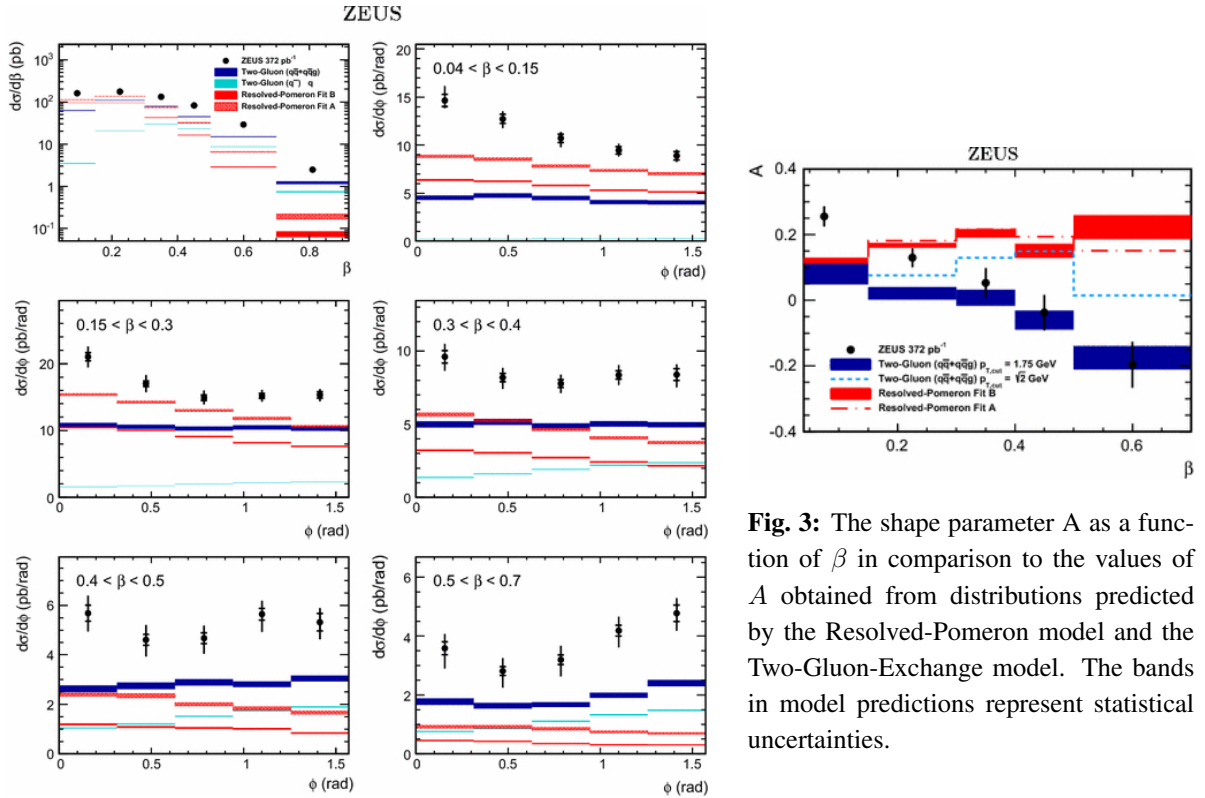


**Fig. 3:** The shape parameter  $A$  as a function of  $\beta$  in comparison to the values of  $A$  obtained from distributions predicted by the Resolved-Pomeron model and the Two-Gluon-Exchange model. The bands in model predictions represent statistical uncertainties.

**Fig. 2:** Differential cross sections  $d\sigma/d\beta$  (in log scale) and  $d\sigma/d\phi$  in bins of  $\beta$  (in linear scale) in comparison to model predictions.

and corresponds to an integrated luminosity of  $372 \text{ pb}^{-1}$ . A clean sample of DIS events with a well-reconstructed electron was selected. Events were accepted if a virtuality of exchanged photon  $Q^2 > 25 \text{ GeV}^2$  and photon-proton center of mass energy  $90 < W < 250 \text{ GeV}^2$ . Diffractive events, characterised by the presence of a large rapidity gap (LRG) between proton beam direction and the hadronic final state, were selected, if the fraction of the proton momentum carried by the diffractive exchange,  $x_{IP} < 0.01$  and  $M_X > 5 \text{ GeV}$ , where  $M_X$  denotes the invariant mass of the hadronic state recoiling against the leading proton. The data were analysed as a function of  $\beta$ .

Jets were found in  $\gamma^* - IP$  centre-of-mass frame with  $z$  axis along virtual photon momentum and  $y$  axis along direction defined by the cross product of virtual photon and scattered lepton momenta, as it shown in Fig. 1. The  $kt$ -cluster algorithm known as the Durham jet algorithm Ref. [2] used allows the association of the individual hadrons with a unique jet on an event-by-event basis.

The differential cross sections  $d\sigma/d\beta$  and  $d\sigma/d\phi$ , as shown in Fig. 2, were compared to MC predictions for the Resolved-Pomeron model Ref. [3] and the Two-Gluon-Exchange model Ref. [4, 5], as implemented in RapGap Monte Carlo generator. The measured absolute cross sections are larger than those of theoretical expectations. Both models predict different shapes in the azimuthal angle  $\phi$  between lepton and jet planes. The shape of the  $\phi$  distributions were parametrized in different intervals of  $\beta$  with the function  $1 + A \cos 2\phi$  as motivated by theory. The  $\phi$  distributions show a significant feature: when going from small to large values of  $\beta$ , the shape varies and the slope of the angular distribution changes sign. The variation of the shape was quantified by fitting a function to the  $\phi$  distributions. The fitted function is predicted by theoretical calculations to be proportional to  $1 + A \cos 2\phi$  and reproduces the data behaviour. The cross section  $d\sigma/d\phi$ , normalised to the integrated cross section, is compared to predictions of the models in Fig. 3. The Two-Gluon-Exchange model predicts reasonably well the measured value of  $A$  for  $\beta > 0.3$ , whereas the Resolved-Pomeron model exhibits a different trend. The Resolved-Pomeron model predicts a negative slope and fails to describe the data, while the Two-Gluon-Exchange model predicts a positive slope, which is consistent with the data. In terms of absolute normalisation, both the Resolved-Pomeron and the Two-Gluon-Exchange models are below the data.

### 3 Measurement of the cross-section ratio $\sigma_{\psi(2S)}/\sigma_{J/\psi(1S)}$

The ratio of the cross sections of the reactions  $\gamma^*p \rightarrow \psi(2S) + Y$  and  $\gamma^*p \rightarrow J/\psi(1S) + Y$ , where  $Y$  denoted either a proton or a low mass proton-dissociation system, was measured with the ZEUS detector in the kinematic range  $2 < Q^2 < 80 \text{ GeV}^2$ ,  $30 < W < 210 \text{ GeV}$  and  $|t| < 1 \text{ GeV}^2$  Ref. [6]. These two charmonium states have the same quark content, different radial distributions of the wave functions and their mass difference is small compared to the HERA centre-of-mass energy. Therefore, the measurement of the ratio of their electro-production cross sections allows perturbative QCD predictions of wave function dependence of the  $c\bar{c}$ -proton cross section to be tested. A suppression of the  $\psi(2S)$  cross section relative to the  $J/\psi(1S)$  is expected, as the  $\psi(2S)$  wave function has a radial node close to the typical transverse separation of the virtual  $c\bar{c}$  pair. The measurement was based on all available

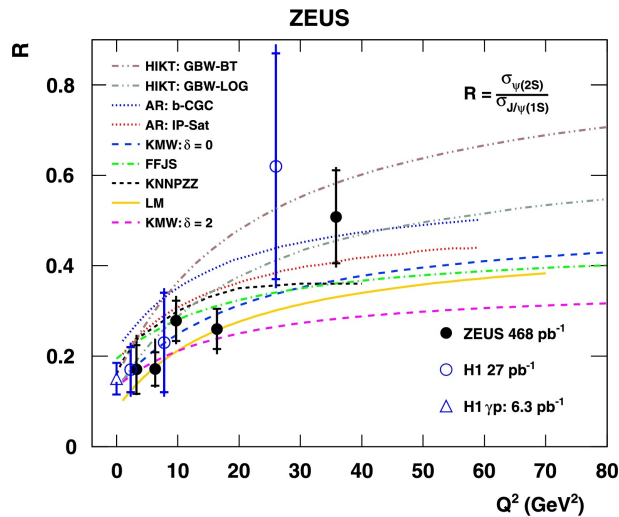


**Fig. 4:** The measured cross section ratio  $R = \sigma_{\psi(2S)}/\sigma_{J/\psi(1S)}$  as a function of photon virtuality  $Q^2$  in comparison to theoretical predictions.

data sample amounting to  $468 \text{ pb}^{-1}$ , which consists of data from 1996-2000 and 2002-2007 running periods. Events were selected with no activity in the central ZEUS detector in addition to signals from the scattered electron and the decay products of the studied mesons. The sample contained exclusive and a small fraction of proton-dissociative events with diffractive masses  $M_Y < 4 \text{ GeV}$  which was assumed

to cancel in the cross section ratio. The decay channels were:  $J/\psi(1S)$ ,  $\psi(2S) \rightarrow \mu^+\mu^-$ , and  $\psi(2S) \rightarrow J/\psi(1S)\pi^+\pi^-$  with the subsequent decay  $J/\psi(1S) \rightarrow \mu^+\mu^-$ . The studied process was simulated with the DIFFVM MC package. The GRAPE package was used for simulating exclusive and Bethe-Heitler dimuon production. The final sample contains  $\sim 2500$   $J/\psi(1S)$  and  $\sim 190$   $\psi(2S)$  events. After correcting for the detector acceptance, efficiency and the branching ratios, the cross section ratio  $R = \sigma_{\psi(2S)}/\sigma_{J/\psi(1S)}$  was determined in bins of  $Q^2$ ,  $W$  and  $|t|$ . No dependence of the ratio on  $W$  and  $|t|$  was found. For the  $Q^2$  dependence of the ratio  $R$  a positive slope is observed. In Fig. 4 the results on  $Q^2$  dependence are shown together with previous H1 measurements Ref. [7, 8]. The H1 Collaboration has found a value of  $R = 0.150 \pm 0.035$  at photoproduction regime ( $Q^2 \approx 0$ ). The HERA data behaviour is consistent with many of the models, which qualitatively reproduce the rise of  $R$  with  $Q^2$  although some of the models are excluded.

#### 4 Exclusive $\rho^0$ meson photoproduction with a leading neutron

The H1 experiment has reported of the measurement of exclusive photoproduction of  $\rho^0$  mesons associated with leading neutrons,  $\gamma p \rightarrow \rho^0 n \pi^+$ , Ref. [9] with the aim to investigate exclusive  $\rho^0$  production on virtual pions in the photoproduction and to extract for the first time experimentally the quasi-elastic  $\gamma p \rightarrow \rho^0 \pi$  cross section. Here, for the  $\rho$  meson photoproduction at a soft scale, Reggy phenomenology is most appropriate to describe the reaction. Figure 5 shows a set of Regge diagrams contributing to the signal (a,b,c) and to background (d) for this process. The pion exchange at the proton vertex is followed by elastic scattering of the pion on the virtual photon emitted from the beam electron,  $\gamma p \rightarrow \rho^0 \pi^+$ . This one-pion-exchange diagram (OPE) dominates at small  $t \rightarrow 0$ , where graphs (b,c) contributing to the scattering amplitude with opposite signs largely cancel. The data sample corresponds to an inte-

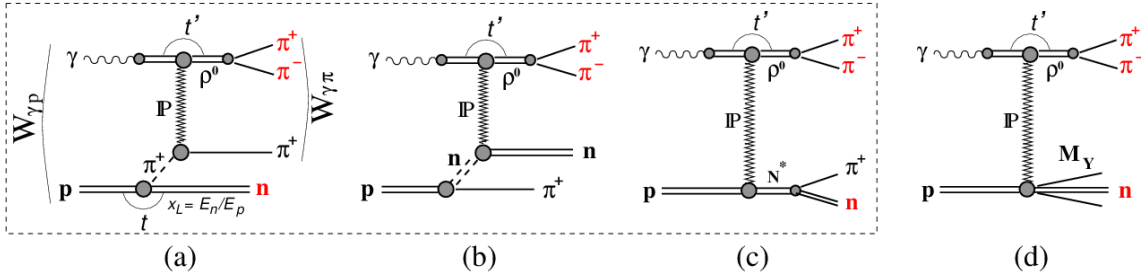


**Fig. 5:** Diagrams for processes contributing to exclusive photoproduction of  $\rho^0$  meson associated with leading neutron. Three processes: pion exchange (a), neutron exchange (b) and a direct pole(c), The diffractive  $\rho^0$  production with proton dissociation (d) is considered as background.

grated luminosity of  $1.16 \text{ pb}^{-1}$  and was collected at  $\sqrt{s_{ep}} = 319 \text{ GeV}$  using a special low multiplicity trigger. Exclusive events are selected containing only two oppositely charged pions from the  $\rho^0$  decay, the leading neutron and nothing else above noise level in detector. This ensure the exclusivity and limits the dissociative background to the range  $M_Y < 1.6 \text{ GeV}$ . The pion from the proton vertex is emitted under very small angle with respect to the proton beam and escapes detection. Signal events (Fig. 5a) are modelled by the POMPYT Monte Carlo generator, in which virtual pion is produced at the proton vertex according to one of the available pion flux parametrizations and then the quasi-elastic scattering process,  $\gamma p \rightarrow \rho^0 \pi^+$ , is generated. Diffractive  $\rho^0$  production with proton dissociation into a system containing a neutron (Fig. 5d) contributes as background and is modelled by the DIFFVM MC generator. This background is subtracted from the data and its fraction in the final data sample is estimated to be  $0.34 \pm 0.05$ .

The cross section of the exclusive reaction  $ep \rightarrow e\rho^0 n \pi^+$  was measured and converted into  $\gamma p$  cross section using the effective photon flux of the Vector Dominance model. The integrated  $\gamma p$  cross

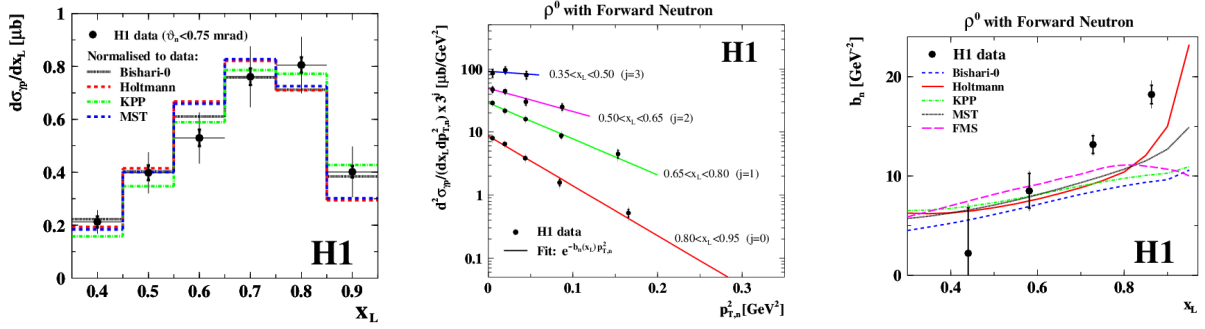


**Fig. 6:** (*left*) Differential cross section  $d\sigma_{\gamma p}/dx_L$  compared to the predictions based on different models for the pion flux. (*middle*) Double differential cross section of neutrons  $d^2\sigma_{\gamma p}/dx_L dp_{T,n}^2$  in the range  $20 < W_{\gamma p} < 100$  GeV fitted with a single exponential function. (*right*) The exponential slope fitted through the  $p_{T,n}^2$  dependence of the leading neutron as a function of  $x_L$  compared to the expectations of several parametrisations of the pion flux within OPE model.

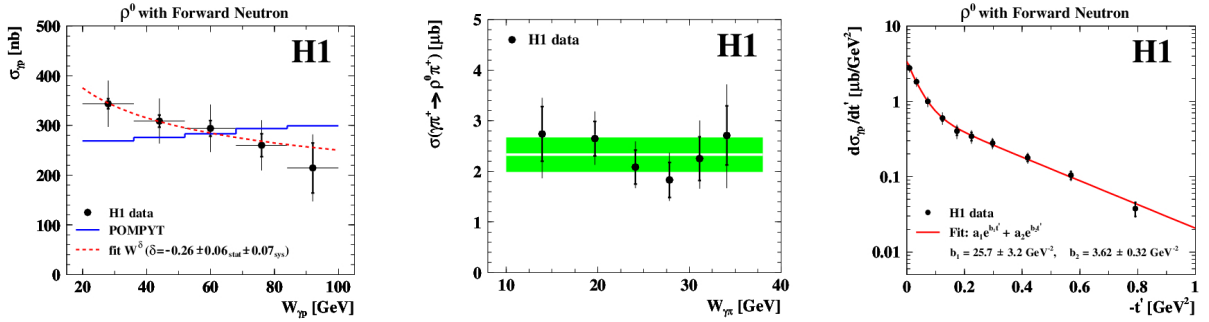


**Fig. 7:** (*left*) Cross section of the reaction  $\gamma p \rightarrow \rho^0 n \pi^+$  as a function of  $W_{\gamma p}$ . (*middle*) Elastic cross section  $\sigma_{el}^{\gamma\pi} \equiv \sigma(\gamma\pi^+ \rightarrow \rho^0\pi^+)$ , extracted in the OPE approximation as a function of the photon-pion energy  $W_{\gamma\pi}$ . (*right*) Differential cross section  $d\sigma_{\gamma p}/dt'$  of  $\rho^0$  meson fitted with the sum of two exponential functions.

section in the kinematic range  $20 < W_{\gamma p} < 100$  GeV,  $0.35 < x_L < 0.95$  and  $\theta < 0.75$  mrad is measured as  $\sigma_{\gamma p} = 310 \pm 6(\text{stat}) \pm 45(\text{sys})$  nb. The differential cross section  $d\sigma_{\gamma p}/dx_L$  compared to the predictions based on different models for the pion flux is shown in Fig. 6. The shape of the  $x_L$  distribution is well reproduced by the pion flux parametrization. The double differential cross section  $d^2\sigma_{\gamma p}/dx_L dp_{T,n}^2$  was measured and fitted with single exponential function and presented in Fig. 6. Steep falling at very high values of  $x_L$  is observed. The exponential slope parameter of the leading neutron  $b_n$  determined from the  $p_{T,n}$  dependence compared to models with various pion flux is shown in Fig. 6. While the shape of the  $x_L$  distribution is well reproduced by most of the pion flux approximations, the  $x_L$  dependence of the  $p_T$  slope of the leading neutron is not described by any of the existing models. The energy dependence of the reaction  $\gamma p \rightarrow \rho^0 n \pi^+$  is presented in Fig. 7. The cross section drops with  $W_{\gamma p}$  in contrast to the POMPYT Monte Carlo expectation, where the whole energy dependence is driven by Pomeron exchange alone. A Regge motivated power law fit  $\sigma \propto W^\delta$  with  $\delta = -0.26 \pm 0.06(\text{stat}) \pm 0.07(\text{sys})$  describes the data. Earlier HERA measurements Ref. [10, 11] have shown that the cross section of the reaction  $\gamma p \rightarrow \rho^0 p$  has another trend and prefers to increase with  $W$  with the Pomeron trajectory  $\delta \approx 0.08$ . The pion flux models compatible with the data in the shape of  $x_L$  distribution are used to extract the photon-pion cross section from  $d\sigma/dx_L$  in the OPE approximation. The results are presented in Fig. 7. Using the pion flux parametrization of the Holtmann model Ref. [12, 13] the elastic  $\gamma\pi$  cross section is determined at the average energy  $\langle W_{\gamma\pi} \rangle \sim 24$  GeV:  $\sigma(\gamma\pi^+ \rightarrow \rho^0\pi^+) = 2.33 \pm 0.34(\text{exp})_{-0.40}^{+0.47}(\text{model}) \mu\text{b}$ . The estimated cross section ratio for the elastic photoproduction of  $\rho^0$  meson on the pion and on the proton, is  $r_{el} = \sigma_{el}^{\gamma\pi}/\sigma_{el}^{\gamma p} = 0.25 \pm 0.06$ . A similar ratio, but for the total cross sections at  $\langle W \rangle = 107$  GeV, has

been estimated by the ZEUS collaboration as  $r_{tot} = \sigma_{tot}^{\gamma\pi} / \sigma_{tot}^{\gamma p} = 0.32 \pm 0.03$  Ref. [14]. Both measured ratios are significantly smaller than the additive quark model predictions. This may be attributed to rescattering, or absorption corrections, which are expected to play an essential role in *soft* peripheral process. For the studied reaction  $\gamma p \rightarrow \rho^0 n \pi^+$  this would imply an absorption factor of  $K_{abs} = 0.44 \pm 0.11$ .

The cross section as a function of the four-momentum transfer squared of the  $\rho^0$  meson,  $t'$ , is shown in Fig. 7. The  $t'$  distribution is fitted with the sum of two exponential functions with different slopes for the low- $t'$  and the high- $t'$  regions, which is typical for double peripheral exclusive reactions. In DPP approach this is due to exchange of two Regge trajectories, Pomeron and pion.

## 5 Summary

A brief review of recent HERA measurements of exclusive processes has been presented. The production of exclusive dijets in deep inelastic  $ep$  scattering was measured for the first time and compared to predictions from models based on different assumptions about the nature of diffractive exchange. The measured cross section ratio of the charmonium states,  $\psi(2S)$  and  $J/\psi(1S)$ , in exclusive deep inelastic electroproduction using full HERA data sample, confirms the expectations of QCD-inspired models of vector-meson production. Photoproduction of exclusive  $\rho^0$  meson associated with a leading neutron measured first time at HERA which allowed the diffractive production of  $\gamma\pi$  scattering to be studied. High accuracy of the presented measurements of the exclusive state production has providing new details to test for QCD theory and experiments at the LHC.

## Acknowledgements

Many thanks to all colleagues in ZEUS and H1 for providing the material in this report.

## References

- [1] ZEUS Collaboration, H. Abramowicz et al., Eur.Phys.J., C **76** (2016) 1, <https://doi.org/10.1140/epjc/s10052-015-3849-z>.
- [2] S. Catani, Y.L. Dokshitzer, M. Olsson, G. Turnock and B.R. Webber, Phys.Lett., B **269** (1991) 432.
- [3] G. Ingelman and P.E. Schlein, Phys.Lett., B **152** (1985) 256.
- [4] J. Bartels, H. Lotter and M. Wuesthoff, Phys.Lett., B **379** (1996) 239, [https://doi.org/10.1016/0370-2693\(96\)00412-1](https://doi.org/10.1016/0370-2693(96)00412-1).
- [5] J. Bartels, H. Jung and M. Wuesthoff, Eur.Phys.J., C **11** (1999) 111.
- [6] ZEUS Collaboration, H. Abramowicz et al., Nucl.Phys., B **909** (2016) 934, <https://doi.org/10.1016/j.nuclphysb.2016.06.010>.
- [7] H1 Collaboration, C. Adloff et al., Phys.Lett., B **421** (1998) 385.
- [8] H1 Collaboration, C. Adloff et al., Eur.Phys.J., C **10** (1999) 373, <https://doi.org/10.1016/j.nuclphysb.2016.06.010>.
- [9] H1 Collaboration, V. Andreev et al., Eur.Phys.J., C **76** (2016) 41, <https://doi.org/10.1007/epjc/s100520050762>.
- [10] ZEUS Collaboration, M. Derrick et al., Phys.Lett., B **293** (1992) 465, [https://doi.org/10.1016/0370-2693\(92\)90914-P](https://doi.org/10.1016/0370-2693(92)90914-P).
- [11] H1 Collaboration, T. Ahmed et al., Phys.Lett., B **299** (1993) 374, [https://doi.org/10.1016/0370-2693\(93\)90277-O](https://doi.org/10.1016/0370-2693(93)90277-O).
- [12] H. Holtmann et al., Phys.Lett., B **338** (1994) 363.
- [13] H. Holtmann, A.Szczurek, J. Speth, Nucl.Phys., A **596** (1996) 631.
- [14] ZEUS Collaboration, S. Chekanov et al., Nucl.Phys., B **637** (2002) 3, [https://doi.org/10.1016/S0550-3213\(02\)00439-X](https://doi.org/10.1016/S0550-3213(02)00439-X).